



*crystals*

IMPACT  
FACTOR  
**2.670**

CITESCORE  
**3.2**

Article

---

# Characterization of Proton-Irradiated Polyaniline Nanoparticles Using Terahertz Thermal Spectroscopy

---

Seung Jae Oh, Yoochan Hong, Ki-Young Jeong, Inhee Maeng, Jin-Suck Suh, Jaemoon Yang and Yong-Min Huh

Special Issue

Investigation of Molecular by Terahertz Spectroscopy


Edited by  
Prof. Dr. Seung Jae Oh



<https://doi.org/10.3390/cryst11070765>

## Article

# Characterization of Proton-Irradiated Polyaniline Nanoparticles Using Terahertz Thermal Spectroscopy

Seung Jae Oh <sup>1</sup>, Yoochan Hong <sup>2</sup>, Ki-Young Jeong <sup>1</sup>, Inhee Maeng <sup>1</sup>, Jin-Suck Suh <sup>1,3,4</sup>, Jaemoon Yang <sup>3,4,5,6,\*</sup>   
and Yong-Min Huh <sup>1,3,4,\*</sup>

- <sup>1</sup> YUHS-KRIBB Medical Convergence Research Institute, College of Medicine, Yonsei University, Seoul 03722, Korea; issac@yuhs.ac (S.J.O.); kiyoung.jeong@gmail.com (K.-Y.J.); INHEEM@yuhs.ac (I.M.); jss@yush.ac (J.-S.S.)
- <sup>2</sup> Department of Medical Devices, Korea Institute of Machinery and Materials (KIMM), Daegu 42994, Korea; ychong1983@kimm.re.kr
- <sup>3</sup> Department of Radiology, College of Medicine, Yonsei University, 50-1 Yonsei-ro, Seodaemun-gu, Seoul 03722, Korea
- <sup>4</sup> Severance Biomedical Science Institute, College of Medicine, Yonsei University, 50-1 Yonsei-ro, Seodaemun-gu, Seoul 03722, Korea
- <sup>5</sup> Department of Radiology, Research Institute of Radiological Science, and Center for Clinical Imaging Data Science (CCIDS), College of Medicine, Yonsei University, Seoul 03722, Korea
- <sup>6</sup> Systems Molecular Radiology Lab, Yonsei University, Seoul 03722, Korea
- \* Correspondence: 177hum@yuhs.ac (J.Y.); ymhuh@yuhs.ac (Y.-M.H.)



**Citation:** Oh, S.J.; Hong, Y.; Jeong, K.-Y.; Maeng, I.; Suh, J.-S.; Yang, J.; Huh, Y.-M. Characterization of Proton-Irradiated Polyaniline Nanoparticles Using Terahertz Thermal Spectroscopy. *Crystals* **2021**, *11*, 765. <https://doi.org/10.3390/cryst11070765>

Academic Editor: Carlo Vicario

Received: 29 May 2021

Accepted: 24 June 2021

Published: 30 June 2021

**Publisher's Note:** MDPI stays neutral with regard to jurisdictional claims in published maps and institutional affiliations.



**Copyright:** © 2021 by the authors. Licensee MDPI, Basel, Switzerland. This article is an open access article distributed under the terms and conditions of the Creative Commons Attribution (CC BY) license (<https://creativecommons.org/licenses/by/4.0/>).

**Abstract:** In this study, we investigated the changes in the molecular structure of polyaniline (PANI) nanoparticles illuminated by a proton beam using terahertz (THz) thermal spectroscopy based on the terahertz time-domain spectroscopy technique. PANI nanoparticles in water were exposed to a proton beam of 35 MeV energy with a particle fluence of  $10^{13}$  particles/cm<sup>2</sup>. The photothermal properties of this solution of PANI nanoparticles were characterized using THz thermal spectroscopy. We measured the changes in the amplitudes of the reflected THz pulses to identify the variations in temperature induced by the photothermal effects of the PANI nanoparticle solution. The amplitude of a reflected THz pulse of the PANI solution not exposed to the proton beam increased when illuminated by an infrared light source, whereas that of THz signals of the PANI solution exposed to the proton beam hardly exhibited any changes. This implies that the molecular structure of PANI nanoparticles can be varied by a proton beam with a particle fluence above  $10^{13}$  particles/cm<sup>2</sup>.

**Keywords:** terahertz spectroscopy; polyaniline; thermal spectroscopy; proton beam

## 1. Introduction

Recent advances in cancer treatment technologies allow direct removal of tumors using various non-contact methods, such as radiation therapy using proton or neutron rays, ultrasound, laser, and thermal therapy [1]. Thermal therapy is known to accelerate therapeutic effects when combined with radiation therapy or chemotherapy [2,3]. Owing to the advances in nanotechnology, tumor removal by localized thermal therapy based on targeted photothermal nanoparticles, wherein the local temperature is increased by laser irradiation, has been increasingly studied [4]. This therapy kills only targeted cancerous tissues rather than normal tissues. When fusion therapy using radiation and localized photothermal treatment is considered, the changes in the material properties of photothermal nanoparticles which could be occurred during radiation therapy must be evaluated because, unlike metal nanoparticles, polymer nanoparticles we used can be distorted and the photothermal efficiency of the nanoparticles could be decreased under the illumination of proton or neutron rays. Polyaniline (PANI) particles, which are conductive polymers, are considered photothermal nano-agents owing to their excellent heat-generating properties under laser irradiation [5–7]. The center of optical absorption wavelength in these particles

is approximately 600 nm in the emeraldine base (EB) state, which shifts to 800 nm in the emeraldine salt (ES) state generated by cation doping. Typically, cancer cells are rich in ionic substances in comparison with normal cells owing to vigorous metabolic activities. When PANI particles are delivered into a cancer cell, it shifts from EB to ES state because of positive ions, such as H<sup>+</sup>, and exhibits photothermal properties in the near-infrared (NIR) wavelength of 800 nm. The thermal conversion efficiency is a major parameter that determines the function of photothermal nanoparticles, and it can be calculated using various temperature measurement techniques. Contact thermometers, such as mercury thermometers, and thermometers using probes provide accurate temperature information. However, directly measuring the area irradiated by the laser is challenging because the laser can interfere with the operation of the thermal sensor. Although infrared thermometers can measure the temperature without contact, they measure only the surface temperature. Therefore, it is difficult to measure the exact temperature at medium depths or the bottom of solutions. Conversely, the wavelength of a terahertz (THz) wave lies in the range of sub-millimeter and millielectronvolt energy, rendering it sensitive to the variations in temperature in water molecules as the THz frequency comprises the recombination and break motion energy of water clusters [8,9]. Therefore, THz time-domain spectroscopy (THz-TDS) can directly not only measure the temperature of the water without contact but also enable to obtain the temperature distribution of layer between the plastic well dish and water under the laser irradiation. Such advantages of THz-TDS allowed the development of THz photothermal imaging, which could perform targeted cancer imaging using targeted nanoparticles [10,11]. In this study, we investigated the thermal properties of PANI nanoparticles with and without proton irradiation using THz thermal spectroscopy to verify its applicability in the non-contact monitoring of photothermal effects.

## 2. Materials and Methods

### 2.1. PANI Particles and Proton Beam Irradiation

We prepared dispersed PANI in water by washing the ES-PANI particles with a substantial amount of deionized water and de-doping the particles with sodium hydroxide to synthesize EB-PANI particles. The solubility of EB-PANI was increased by coating the synthesized PANI particles with Tween 80. Additionally, the MC-50 cyclotron of Korea Institute of Radiological and Medical Sciences (KIRAMS) was used as a proton beam source [12]. The synthesized PANI particle solution was enclosed in an aluminum case and exposed to protons. The irradiation energy of 40 MeV decreased to 35 MeV when passed through 2 mm of aluminum, and the PANI solution samples were exposed to the proton beam with a fluence of  $1 \times 10^{13}$  particles per unit cm<sup>2</sup>. The ultraviolet (UV) and visible spectrum of samples were measured in the 400–1000 nm range using an ultraviolet-visible (UV-Vis) spectrometer (UV-1800, Shimadzu). Experiments were implemented 24 h after removal of the residual radioactivity of samples.

### 2.2. Terahertz Thermal Spectroscopy

We used an in-house reflection-type THz-TDS system, wherein a Ti-sapphire femtosecond laser with a center wavelength of 808 nm and a pulse width of 80 fs was used to generate and detect THz pulses. The femtosecond laser was divided using a beam splitter, and the two beams were irradiated to the generation and detection antennas, as illustrated in Figure 1a. An electric potential of 90 V was applied between the lines of the coplanar antenna to accelerate the electron-hole pairs induced by the pumped laser. The generated THz pulses that passed through parabolic mirrors were focused on the sample. The reflected pulses passing through the parabolic mirror were convoluted with another pulse laser on the dipole antenna. We used a continuous-wave (CW) NIR laser of wavelength 808 nm to induce the photothermal effect on the nanoparticles. The CW-NIR laser overlapped with the THz pulse beam focused on the sample with a beam diameter of 2 mm, as depicted in Figure 1b. The PANI solution was placed into a polystyrene well plate, SPL (32096), which was transparent to the terahertz beam and CW-NIR laser.

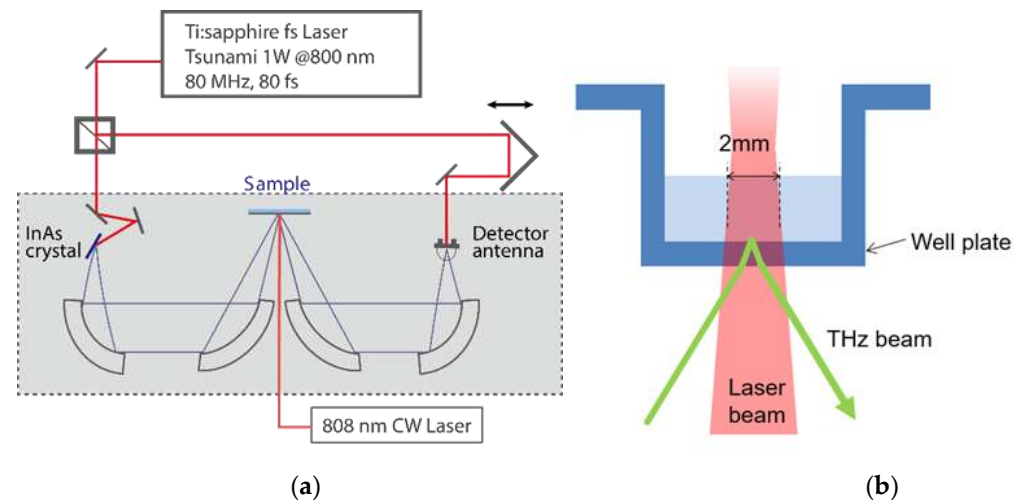


**Figure 1.** (a) Terahertz (THz) thermal spectroscopy and (b) a sample schematic.

### 3. Results

#### 3.1. Visible Spectroscopy of PANI

Typically, PANI conductive polymers are doped or protonated in an acid, such as hydrochloric acid or sulfuric acid. We transformed the PANI particles from EB to ES state by adding 1M HCl solution. The -N- part of the EB state was doped with  $H^+$  ions in the HCl solution to modify it to the -NH- of the ES state. The red line in Figure 2 depicts the absorption spectrum of EB and ES states of PANI without proton irradiation. The absorption spectrum varied with the change in the state of PANI.

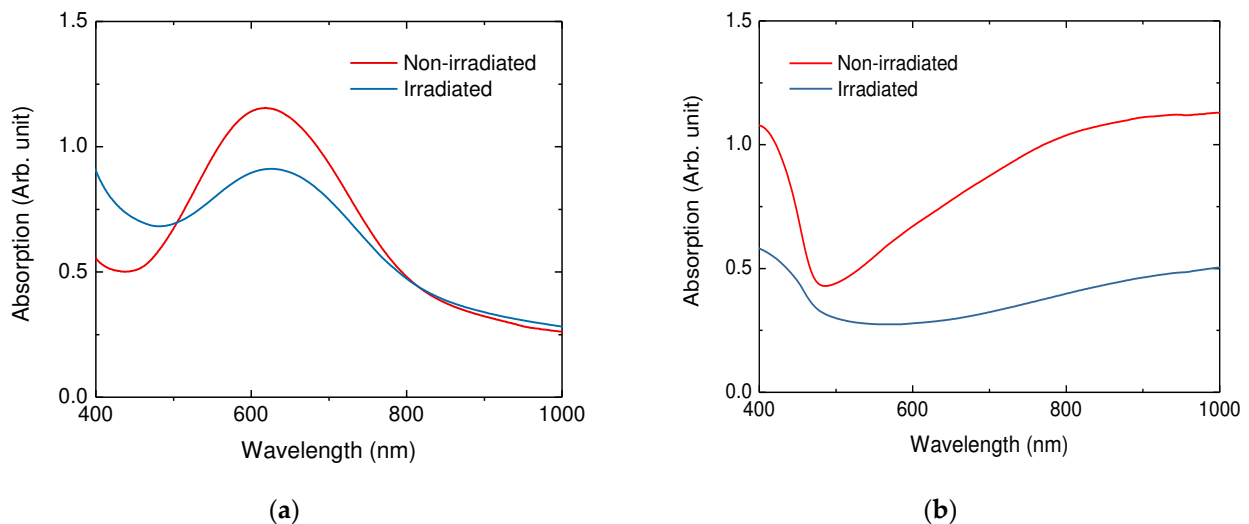


**Figure 2.** UV–visible spectrum of polyaniline (PANI) solution. Spectra of (a) emeraldine base (EB) PANI and (b) emeraldine salt (ES) PANI. The red and blue lines indicate the spectrum before and after proton exposure with a fluence of  $10^{13}$  N/cm<sup>2</sup>, respectively.

The peak position of the wavelength shifted from 600 to 800 nm, and the bandwidth of the envelope expanded owing to the transformation from EB to ES state. However, this typical spectrum transformation was modified by proton irradiation. When the PANI nanoparticles were exposed to a proton beam of  $10^{13}$  N/cm<sup>2</sup> fluence at 35 MeV of energy, the peak intensity at the wavelength of 600 nm of the EB state decreased, and the absorption level of the spectrum in the ES state decreased to a level lower than that observed before the proton beam exposure, as shown in Figure 2. The UV–Vis spectroscopy result implies that the proton irradiation distorted the molecular structures of the PANI particles. We used

THz thermal spectroscopy to investigate the degradation of the photothermal response due to changes in the molecular structure of PANI nanoparticles.

### 3.2. THz Thermal Spectroscopy of PANI

We measured the THz pulses reflected from the plastic well containing the ES-PANI solution. The measured THz time-domain waveform comprised two pulses: the first was the signal reflected from the layer between air and the surface of the plastic well, and the second was the signal reflected from the layer between the plastic well and ES-PANI solution. The former pulse was nearly unaffected by the increase in the power of the CW-NIR laser, whereas the peak amplitude value of the second pulse increased by 170 s. These results showed that CW-NIR radiation only raised the temperature of water with ES-PANI nanoparticles and did not respond with plastic well plates [6,10]. As the temperature of the solution increased, the refractive index of the THz range increased, which in turn increased the reflected signal amplitude. Figure 3 depicts the time- and frequency-domain waveforms of the second pulse based on the CW-NIR laser power after 170 s of laser irradiation. The change in the THz pulse was not observed when the power of CW-NIR laser irradiation was 1 W, but the amplitudes of THz pulses increased when the laser power exceeded 1 W.

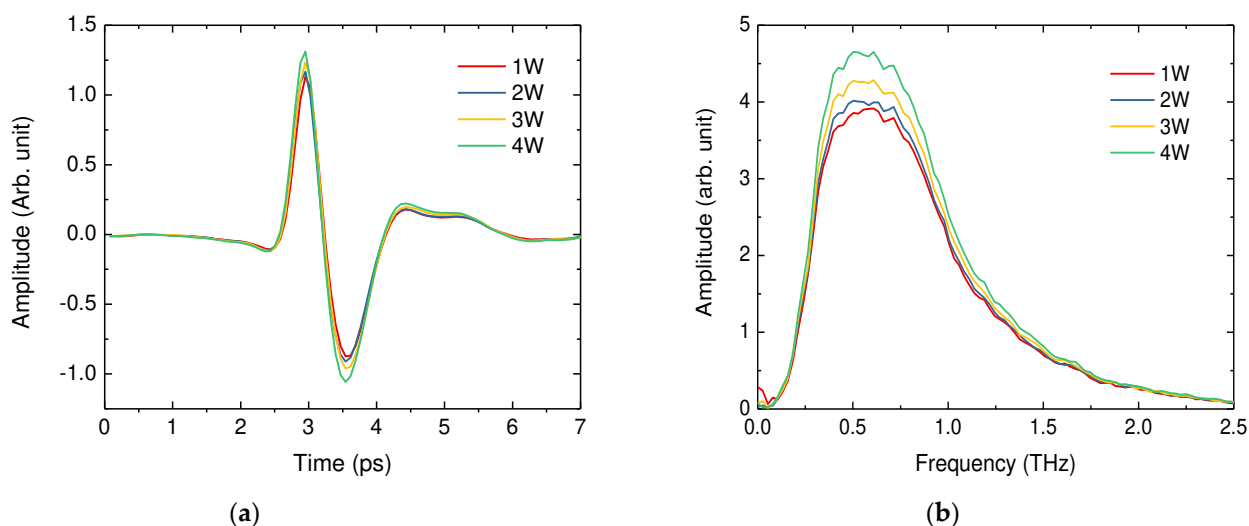


**Figure 3.** Reflected terahertz waveform of water-dispersed emeraldine salt polyaniline (ES-PANI) nanoparticles based on the applied laser power. (a) Time- and (b) frequency-domain waveforms. The legend indicates the power of the continuous-wave near-infrared (CW-NIR) laser with a wavelength of 808 nm. The terahertz waveform without CW-NIR irradiation is identical to the waveform of 1 W.

Figure 4 illustrates the time sequencing data of the peak-to-peak values of THz pulses of EB- and ES-PANI solutions based on the applied CW-NIR laser power. When the CW-NIR laser was illuminated on the PANI solution after 10 s, the modulation depth of the peak-to-peak values of THz pulses reflected from the EB-PANI solution was lower than that of the ES-PANI solution. As depicted in Figure 4a, the modulation ratio of THz pulses of EB-PANI did not exceed 10% even when irradiated for 170 s by 4 W of CW-NIR laser power. However, the ES-PANI solution instantly responded to the CW-NIR laser irradiation (Figure 4b). As can be seen from the figure, the THz pulse intensity increased rapidly to 4% for the initial 2 s and then increased by 20% for 170 s at a CW-NIR laser power of 4 W. We observed that the rate of change in the THz pulse intensity was proportional to the intensity of the laser. When the CW-NIR lasers were irradiated on the sample with 3 and 2 W, the THz pulse intensities increased by 12 and 7%, respectively, after 170 s. However, both EB- and ES-PANI solutions remained unaffected when irradiated with a low laser power of 1 W. This result implies that the THz-TDS system can effectively evaluate the photothermal effect of nanoparticles based on the generated THz pulses. In particular, the

rapid increase in the temperature curve at the border of the well plate and solution is rarely observed by other techniques, such as thermocouples and infrared thermometers which can just observe the surface temperature of plastic well, diffused from the solution.

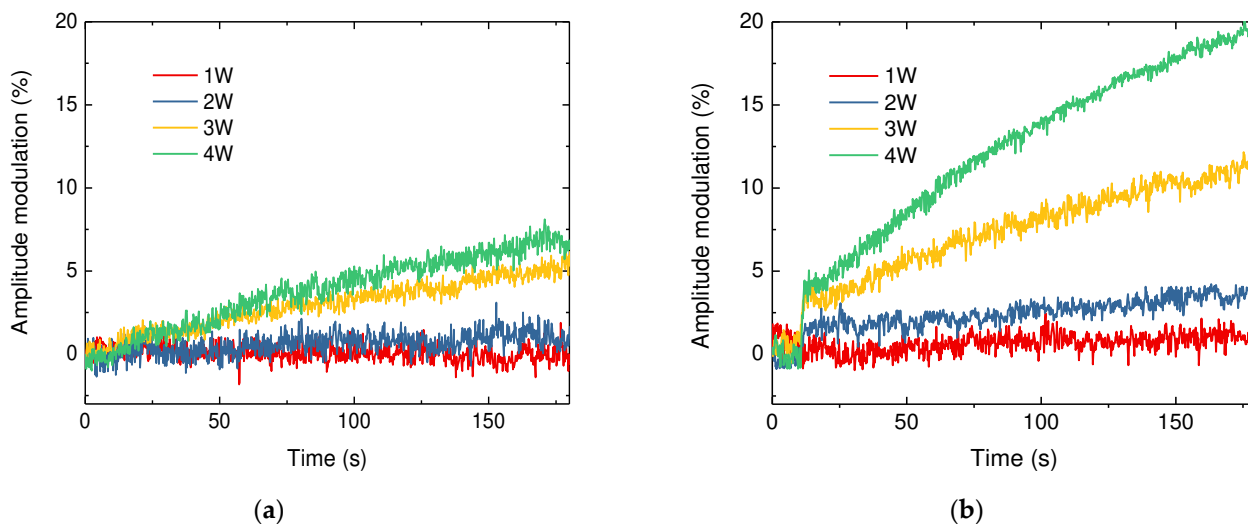


**Figure 4.** Time sequencing data of the peak-to-peak values of terahertz pulses of (a) emeraldine base (EB) and (b) emeraldine salt (ES) polyaniline (PANI) solutions based on the power of the continuous-wave near-infrared (CW-NIR) laser. The laser was irradiated on the solution after 10 s. The legend indicates the power of the CW-NIR laser with a wavelength of 808 nm.

The photothermal properties of PANI nanoparticles exposed to the proton beam were evaluated using THz thermal spectroscopy. The prepared EB-PANI solution was exposed to a proton beam of 35 MeV energy and a particle fluence of  $10^{13}$  N/cm<sup>2</sup>. Additionally, EB-PANI was transferred to the ES state using 1M HCl. This process corresponds to the application of EB-PANI to cancer cells in a living body, wherein the pH values are higher than those of normal cells [5]. Figure 5 depicts the time sequencing data of the peak-to-peak values of THz pulses of EB- and ES-PANI solutions exposed to the proton beam based on the power of the CW-NIR laser. Unlike the results of the EB-PANI solution without proton exposure (Figure 4a), the modulation depth of the peak-to-peak values of the THz pulse reflected from the EB-PANI solution when the CW-NIR laser was irradiated after 10 s was rarely observed at different laser powers (Figure 5a). The photothermal efficiency of the ES-PANI solution, obtained by adding HCL to EB-PANI, was lower when the solution was subjected to proton exposure than that observed without proton beam exposure.

Furthermore, the THz pulse modulation ratio of EB-PANI irradiated by the proton beam was reduced to half of that observed in the absence of the proton beam under identical CW-NIR laser powers, as depicted in Figure 5b. This corresponds to the UV-Vis absorption spectroscopy result presented in Figure 2b, wherein the UV-Vis absorption spectrum of the irradiated ES-PANI solution at 808 nm was reduced. This result implies that the proton illumination modified the molecular structure of PANI and reduced the probability of PANI particles being doped by proton beam irradiation. Therefore, both the absorbed CW-NIR laser in PANI nanoparticles and the photothermal activity in the CW-NIR laser at a wavelength of 808 nm were reduced. Thus, we experimentally proved that, in fusion therapy combining a proton beam with a fluence above  $10^{13}$  protons per unit cm<sup>2</sup> and photothermal therapy based on PANI nanoparticles, the photothermal therapy must precede the proton therapy.

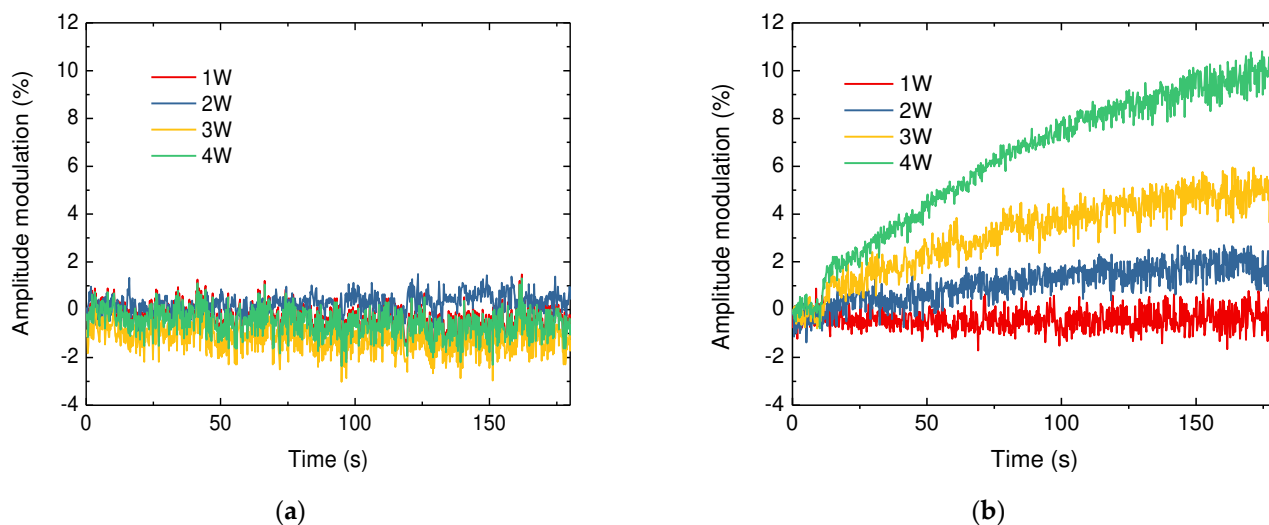


**Figure 5.** Time sequencing data of the peak-to-peak values of terahertz pulses of (a) emeraldine base (EB) and (b) emeraldine salt (ES) polyaniline (PANI) solutions exposed to a 35 MeV energy proton beam with a fluence of  $10^{13}$ . The laser was irradiated on the solution after 10 s. The legend indicates the power of the continuous-wave near-infrared (CW-NIR) laser with a wavelength of 808 nm.

#### 4. Conclusions

We investigated the changes in the photothermal properties of PANI nanoparticles under the illumination of a proton beam using THz thermal spectroscopy based on THz-TDS. We exposed a solution of PANI nanoparticles to a 35 MeV energy proton beam with a particle fluence of  $10^{13}$  particles/cm<sup>2</sup>. The time sequencing temperature variations induced by the photothermal properties of PANI solutions were observed using THz thermal spectroscopy. The amplitude of the reflected THz pulse of the PANI solution without exposure to the proton beam increased under infrared illumination, whereas the PANI solution exposed to the proton beam exhibited minor changes in the THz signal. This implies that the molecular structure of a PANI nanoparticle can be altered by a proton beam with a particle fluence above  $10^{13}$  particles/cm<sup>2</sup>. Thus, we experimentally verified that THz thermal spectroscopy aids in the non-contact monitoring of photothermal effects by measuring the modulation depth to the real temperature increase in the solution.

**Author Contributions:** Conceptualization, S.J.O. and K.-Y.J.; methodology, Y.H. and J.Y.; software, I.M.; validation, J.-S.S.; investigation, Y.-M.H.; writing—original draft preparation, S.J.O.; visualization, I.M. All authors have read and agreed to the published version of the manuscript.

**Funding:** This research was funded by the Technology development Program (S2956549), funded by the Ministry of SMEs and Startups (MSS, Korea), and the Basic Science Research Program through the National Research Foundation of Korea (NRF), funded by the Ministry of Education (NRF-2020R111A1A01075275).

**Acknowledgments:** The authors thank the Korea Institute of Radiological and Medical Sciences (KIRAMS) for assistance with the MC-50 cyclotron.

**Conflicts of Interest:** The authors declare no conflict of interest.

#### References

- Kim, J.H.; Hahn, E.W.; Ahmed, S.A. Combination hyperthermia and radiation therapy for malignant melanoma. *Cancer* **1982**, *50*, 478–482. [\[CrossRef\]](#)
- Overgaard, J. Simultaneous and sequential hyperthermia and radiation treatment of an experimental tumor and its surrounding normal tissue in vivo. *Int. J. Radiat. Oncol. Biol. Phys.* **1980**, *6*, 1507–1517. [\[CrossRef\]](#)
- Overgaard, J. The current and potential role of hyperthermia in radiotherapy. *Int. J. Radiat. Oncol. Biol. Phys.* **1989**, *16*, 535–549. [\[CrossRef\]](#)

4. Chatterjee, D.K.; Diagardjane, P.; Krishnan, S. Nanoparticle-mediated hyperthermia in cancer therapy. *Ther. Deliv.* **2011**, *2*, 1001–1014. [[CrossRef](#)] [[PubMed](#)]
5. Yang, J.; Choi, J.; Bang, D.; Kim, E.; Lim, E.-K.; Park, H.; Suh, J.-S.; Lee, K.; Yoo, K.-H.; Kim, E.-K.; et al. Convertible organic nanoparticles for near-infrared photothermal ablation of cancer cells. *Angew. Chem. Int. Ed.* **2011**, *50*, 441–444. [[CrossRef](#)] [[PubMed](#)]
6. Hong, Y.; Cho, W.; Kim, J.; Hwang, S.; Lee, E.; Heo, D.; Ku, M.; Suh, J.-S.; Yang, J.; Kim, J.H. Photothermal ablation of cancer cells using self-doped polyaniline nanoparticles. *Nanotechnology* **2016**, *27*, 185104. [[CrossRef](#)] [[PubMed](#)]
7. Bae, S.R.; Choi, J.; Kim, H.O.; Kang, B.; Kim, M.H.; Han, S.; Noh, I.; Lim, J.-W.; Suh, J.-S.; Huh, Y.-M.; et al. Pseudo metal generation via catalytic oxidative polymerization on the surface of reactive template for redox switched off–on photothermal therapy. *J. Mater. Chem. B* **2015**, *3*, 505–513. [[CrossRef](#)] [[PubMed](#)]
8. Son, J.-H. *Terahertz Biomedical Science and Technology*; CRC Press: Boca Raton, FL, USA, 2014.
9. Son, J.-H. Terahertz electromagnetic interactions with biological matter and their applications. *J. Appl. Phys.* **2009**, *105*. [[CrossRef](#)]
10. Oh, S.J.; Kang, J.; Maeng, I.; Suh, J.S.; Huh, Y.M.; Haam, S.; Son, J.-H. Nanoparticle-enabled terahertz imaging for cancer diagnosis. *Opt. Exp.* **2009**, *17*, 3469–3475. [[CrossRef](#)] [[PubMed](#)]
11. Oh, S.J.; Choi, J.; Maeng, I.; Park, J.Y.; Lee, K.; Huh, Y.M.; Haam, S.; Suh, J.-S.; Son, J.H. Molecular imaging with terahertz waves. *Opt. Exp.* **2011**, *19*, 4009–4016. [[CrossRef](#)] [[PubMed](#)]
12. Kh, M.U.; Kim, G.; Kim, K.; Kassim, H.B.A.; Nikouravan, B. Investigations of proton beam energy of the MC-50 cyclotron at KIRAMS. *Int. J. Phys. Sci.* **2011**, *6*, 3168–3174.